International Journal of Heat and Mass Transfer 52 (2009) 2324–2334

Contents lists available at ScienceDirect

International Journal of Heat and Mass Transfer

journal homepage: www.elsevier.com/locate/ijhmt

Marangoni condensation heat transfer of water–ethanol mixtures on a vertical surface with temperature gradients

JinShi Wang, JunJie Yan *, ShenHua Hu, JiPing Liu

State Key Laboratory of Multiphase Flow in Power Engineering, Xi'an Jiaotong University, Xi'an 710049, China

ARTICLE INFO

Article history:
Received 8 January 2008
Received in revised form 7 November 2008
Available online 7 January 2009

Keywords:
Marangoni condensation
Temperature gradients
Heat transfer coefficient
Concentration gradients

ABSTRACT

Marangoni condensation heat transfer of water–ethanol mixture vapours was investigated experimentally on a vertical surface with large and nonhomogeneous temperature gradients. The heat transfer investigation showed that the local heat transfer coefficients (HTCs) were varied along the surface for the nonhomogeneous temperature gradients on condensing surface. At the position with greater local temperature gradient, the HTC was higher. The highest HTC existed at the ethanol vapour concentration (EVC) of 1% and the HTC decreased with the increase of EVC when the EVC was more than 2%. Compared to the solutal Marangoni condensation, which was only driven by concentration gradients, owing to the effect of temperature gradients, the present heat transfer was enhanced by 25–100% for the mixture vapours ($C_V < 5\%$ and $C_V = 50\%$) and pure steam, and by 0–50% for the other mixture vapours ($5\% \leqslant C_V < 20\%$). In addition, the effect of vapour velocity and pressure was confirmed to be positive to condensation heat transfer. The preliminary analysis illustrated that, for a positive system with a volatile component, under the coaction of concentration and temperature gradients, the surface tension gradients on the saturated condensate surface became greater, leading to the Marangoni condensation heat transfer to be further enhanced. Meanwhile, the visual observations indicated that condensation modes greatly depended on EVC and vapour-to-surface temperature difference (ΔT).

1. Introduction

When the binary mixture vapours of a positive system, e.g., water–ethanol mixtures, condenses on a solid surface, irregular modes of condensate of uneven thickness appear, such as dropwise condensation. As Marangoni effect is responsible for the dropwise condensation, the phenomenon is called Marangoni condensation or Marangoni pseudo-dropwise condensation. In 1961 Mirkovich and Missen [1] firstly discovered this non-filmwise condensation phenomenon for binary vapours, and compared HTCs for the various types of binary vapours condensation in 1963 [2]. In 1968 Ford and Missen [3] demonstrated a criterion for film instability by an inequality, and established a sign convention $d\sigma/db$ by $d\sigma/db \leqslant 0$ for stable and $d\sigma/db > 0$ for unstable, where σ was the surface tension and b was film thickness. A positive system, where the surface tension of the highboiling-point component was larger than that of the lowboiling-point component, coagulated on a solid surface, the sign convention $d\sigma/db$ was positive and the condensation film would be unstable. Fujii et al. [4] presented an experimental study of condensation of water and ethanol mixtures on a horizontal tube. Their group reported five condensation modes: drop, streak, ring, smooth film and wavy film. For vapour mixtures having ethanol concentrations of 0–20%, the condensation HTC was less than that of pure steam. In 1994 Hijikata et al. [5] theoretically and experimentally investigated the condensation mechanisms of water–ethanol mixture on a flat plate by instability analysis, and found that the values of HTCs were relatively low. All the studies above reported that the HTC of binary vapours was less than or equal to that of pure steam.

On the other hand, in 1997 Morrison and Deans [6] studied the condensation of water–ammonia mixtures on the outside of a smooth horizontal tube. Their results showed that condensation heat transfer was enhanced by as much as 13% when the vapour concentration of ammonia in steam was in the range of 0.23–0.88%. The paper by Philpott and Deans in 2004 [7] reported that on the rates of condensation heat transfer for weak ammonia–water mixtures in a horizontal, shell and tube condenser, the average condensation heat transfer for the condenser was enhanced by up to 14%, for inlet ammonia concentrations in the range of 0.2–0.9%. Furthermore, local enhancement of the condensation heat transfer reached up to 34% when the local bulk vapour concentrations of ammonia ranged from 0.2% to 2%. In recent years Utaka and coworkers performed a series of experiments on Marangoni condensation for water–ethanol mixtures on a small vertical plane. They first achieved several times heat transfer enhancement and found the HTC revealed nonlinear characteristics with peak values with the increase of surface subcooling. They systematically

* Corresponding author. Tel.: +86 29 82665741; fax: +86 29 82675741.
E-mail address: yanjj@mail.xjtu.edu.cn (J. Yan).

0017-9310/$ - see front matter © 2008 Elsevier Ltd. All rights reserved.
doi:10.1016/j.ijheatmasstransfer.2008.11.011

Nomenclature

b	film thickness (μm)
C	ethanol mass concentration in solution (%)
C_V	ethanol vapour mass concentration in mixture vapour (%)
F	ratio of heat transfer coefficient
h	heat transfer coefficients (kW m^{-2} K^{-1})
$\bar{h}$	mean heat transfer coefficient (kW m^{-2} K^{-1})
l	distance (mm)
P	vapour pressure (kPa)
q	heat flux (kW m^{-2})
$\bar{q}$	mean heat flux (kW m^{-2})
r_e	latent heat of ethanol (kJ kg^{-1})
r_{mix}	latent heat of mixture (kJ kg^{-1})
r_w	latent heat of water (kJ kg^{-1})
T	temperature (K)
T_V	vapour temperature (K)
U	vapour velocity (m s^{-1})

Greek symbols

Δh	heat transfer coefficient difference (kW m^{-2} K^{-1})
ΔT	vapour-to-surface temperature difference (K)
Δt	local temperature difference (K)
$\overline{\Delta T}$	mean vapour-to-surface temperature difference (K)
$\Delta\sigma$	surface tension difference (mN m^{-1})
λ	thermal conductivity (kW m^{-1} K^{-1})
σ	surface tension (mN m^{-1})
τ	time (s)
ϕ	heat transfer rate (kW)

Subscript

a–f	different location in the plate
i, j	tab
max	peak points of condensation curves
sat	saturation
w, n, e, s	direction

investigated the dependence of HTCs on surface subcooling [8], vapour velocity [9] and EVC [10]. The HTC was found to be relatively low at small surface subcooling and subsequently to increase steeply before decreasing again. The effect of vapour velocity was to raise HTC. The maximum HTC in the condensation characteristic curves appeared at an ethanol vapour mass fraction of approximately 1% and then HTCs decreased with increasing EVCs. Compared to pure steam, the condensation heat transfer was enhanced approximately 2–8 times. Murase et al. [11] studied the Marangoni condensation using a horizontal condenser tube. The results showed the same trends as those found by Utaka for vertical surfaces. Differences in detail could be explained by geometry considerations and strong dependence of HTC on ΔT and vapour velocity, both of which varied around the perimeter of the horizontal tube. In addition, Yan et al. [12,13] investigated the effect of vapour pressure on Marangoni condensation for water–ethanol vapours. The condensation modes took different appearances under different vapour pressures. The data showed that the HTC increased with the increasing pressure and the promotion effect was significant at low EVCs.

The Marangoni effect is caused by surface tension gradients on the free surface. It can be the result of concentration and/or temperature gradients. In the case of concentration gradients, the effect is called the solutal Marangoni effect. When temperature gradients are responsible for the Marangoni effect, the effect is frequently called thermocapillarity. The previous condensation studies above almost only focused on the effect of concentration gradients, known as so-called solutal Marangoni condensation. In their studies, the experiments were carried out on flat plates or tubes, and the temperature of their condensing surfaces was uniform on macroscale. For the binary mixture vapours and the uniform temperature on the condensing surface, the original intention of the previous works was to use the solutal effect to obtain the pseudo-dropwise condensation. But in the current heat-exchanger field, in order to get more heat transfer, lots kinds of fins were adopted in the heat exchangers. The actual cooling surface was not always flat and the temperature field was always uniform. It was necessary to study the condensation rules on a surface with temperature gradients. For the temperature gradients on the condensing surface in the binary mixture vapours condensation, the original intention of this condensation was to use the solutal effect and thermal effect to obtain the pseudo-dropwise condensation. There were only few references concerned with the condensation on a surface with temperature gradients for mixture vapours. Utaka and Kamiyama [14] studied the spontaneous movement of condensate drops by applying bulk temperature gradient on the heat transfer surface in Marangoni condensation. As a result of experiment using water–ethanol vapour mixture, the movement of droplets from low temperature-side to high temperature-side could be observed on the heat transfer surface arranged horizontally. Hu et al. [15] investigated the Marangoni condensation on an oblique plate and primarily studied the effect of temperature gradients on the heat transfer flux. The temperature gradients on condensing surface were thought to be small, continuous and homogeneous. The mean HTC could be augmented as much as 15% compared with the literature under similar experimental conditions. From this research it could be concluded that the magnitude of temperature gradient would affect the efficiency of heat transfer enhancement. In other words, greater temperature gradients may promote higher heat transfer. Also, the nonhomogeneous temperature gradients on the condensing surface may create stronger disorder and stronger Marangoni convection. The direct result may be a further heat transfer enhancement. So it is necessary to investigate the Marangoni condensation on surfaces with other style of temperature gradients. The purpose of this paper is to study the Marangoni condensation heat transfer characteristic on a vertical surface with larger and nonhomogeneous temperature gradients deeply.

2. Experimental apparatus and methods

2.1. Experiment apparatus

As mentioned in Section 1, in engineering application, many kinds of fins, such as taper fin and flat fin, have been designed in the heat exchangers to enhance heat transfer. The oblique plate in the Hu et al. [15] is just thought to be the application of taper fin. The application of flat fin has not been reported in Marangoni condensation researches. A copper plate, shown in Fig. 1(a), was devised specifically for getting a condensing surface with temperature gradients as described in Section 1, thought to be the application of flat fin. The condensing surface had an area of 25 mm × 40 mm. One typical temperature field of cross section is shown in Fig. 2(a), calculated by a numerical simulation. As seen in Fig. 2(a), the temperature field was serrated. The temperature of condensing surface was nonhomogeneous, but symmetrical. At

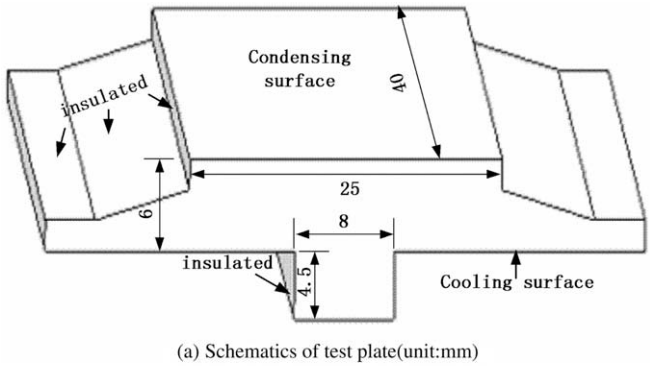

(a) Schematics of test plate(unit:mm)

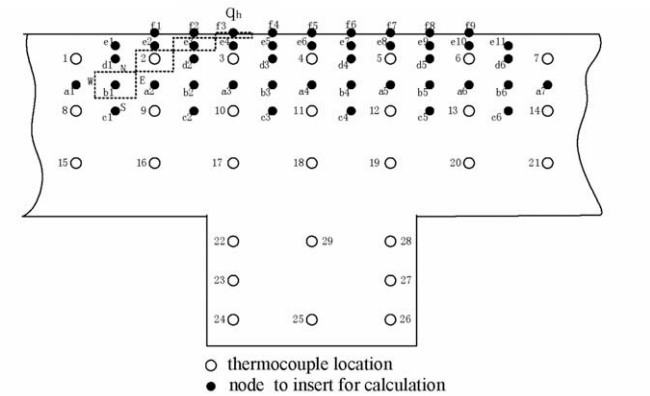

(b) Schematics of thermocouple distribution

Fig. 1. Schematics of test plate and thermocouple distribution in cross section.

the position of the middle line the temperature was highest, while at the edge the temperature was lowest. The local temperature difference on the condensing surface was also nonhomogeneous. The largest temperature difference on the whole surface was up to 6 K. Also shown in Fig. 2(b) is the temperature field of the plate in Ref. [15], calculated under the same condition. From the comparison of the two figures, it could be seen that the temperature gradients on the present condensing surface were nonhomogeneous and larger.

The test apparatus, shown schematically in Fig. 3, consisted of three closed loops: the water–ethanol mixture vapour loop, the impinging jet cooling water loop and the auxiliary cooling water loop. Water–ethanol mixture vapour was generated in an electrically heated boiler (maximum power 12 kW), and then was led into the upper entrance of a vertical rectangular cross-sectional duct, where mixture vapour partly condensed on the vertical surface of the copper plate. The cross section of the duct was 1100 mm^2. The excess vapour flowed into the condenser and was cooled completely. Before returning to the boiler, the condensate was measured in a calibrated flowmeter. Combined the mass flow rate with the cross-sectional area and condensation pressure measured by a pressure transducer in the condensing chamber, a vapour velocity passing through the condensing surface could be calculated. Intending to minimize the effect of non-condensable gas, a vacuum pump near the outlet of the auxiliary condenser continuously worked. The inlet of the vacuum pump was cooled by cooling water to maintain a constant ethanol concentration in the vapour mixture. In the loop of impinging jet cooling water, the cooling water was kept in a cooling water tank where the water was heated continuously and slowly by electrical heaters and was pumped to cool the mixture vapour on the backside of the heat transfer plate. In order to provide high-cooling intensity uniformly, impinging water was jetted from a bundle of thin tubes. The auxiliary cooling water loop was set to cool the excess vapour and control the vapour pressure. By controlling the mass flow rate of cooling water through the condenser, the pressure in the test was adjusted.

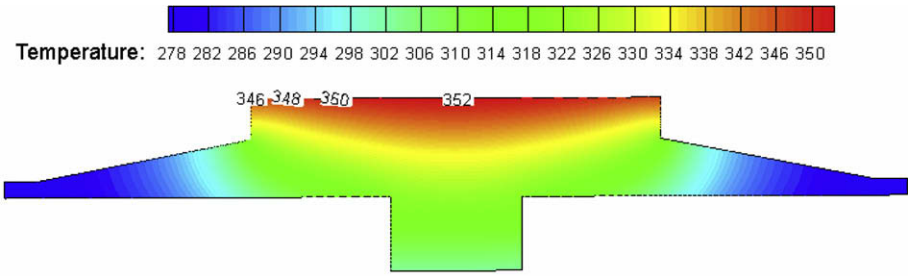

(a) Temperature field of present plate

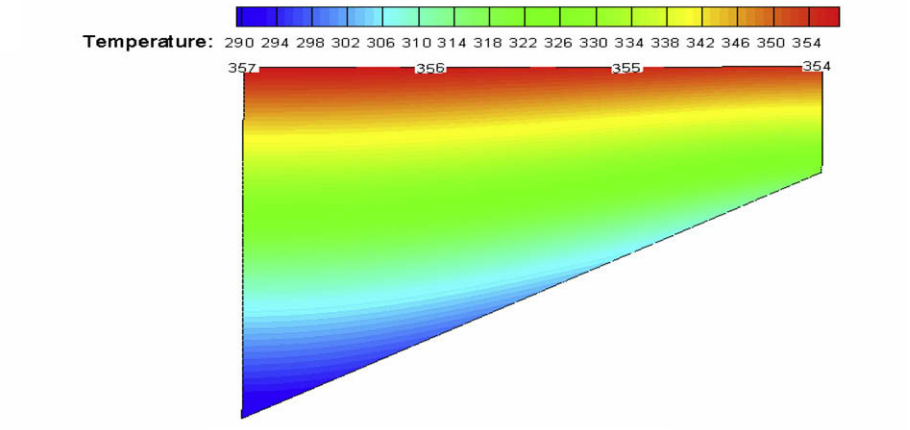

(b) Temperature field of the plate in reference[15]

Fig. 2. One typical temperature field of cross section of test plate.

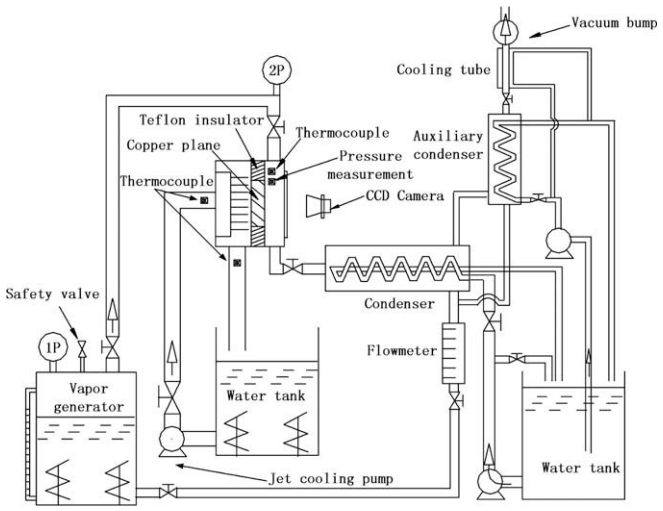

Fig. 3. Schematics of apparatus.

After the vapour condition reached the steady state, the condensation characteristic curves were measured continuously using a quasi-steady measurement in which the temperature of the cooling water was changed very slowly for a fixed concentration, fixed velocity and fixed vapour pressure. The aspect of condensate was observed and recorded through the glass window of the condensing chamber using a CCD camera (REDLAKE® MotionScope2000).

2.2. Methods of measurement

2.2.1. The measurement of vapour pressure

The vapour pressure was measured by a pressure transducer (MSI®US686-002BA, accuracy of 0.1%), and the pressure tap was set up on the duct wall beside the condensate surface as shown in Fig. 3. During the experiment the pressure was adjusted by controlling the mass flow rate of cooling water.

2.2.2. The measurement of vapour velocity

The vapour velocity was measured by two methods as follows:

(1) *Power Calculation Method:* The mass flow rate of the vapour was calculated by the latent heat of vapourization of mixtures r_{mix} and the electric power of heaters in vapour generator, the latent heat of vapourization of mixtures r_{mix} could be calculated as:

$$r_{mix} = r_e \cdot C + r_w \cdot (1 - C) \quad (1)$$

where C was the ethanol mass concentration in the mixture solution. Combining this with the cross-sectional area and condensation pressure, the vapour velocity could be calculated.

(2) *Flowmeter Method:* The mass flow rate of the vapour passing through the condensing surface was measured by flowmeter behind the condenser.

During the experiment, the initial vapour velocities were given as 3 m s^{-1}, 4 m s^{-1} and 6 m s^{-1}, and then the required electric power of heaters was calculated. Finally, the real vapour velocity was calibrated by the second method. The difference between these two methods was less than 5%.

2.2.3. The measurement of vapour concentration

The generated vapour concentration during the boiling process was found to coincide with that given by the vapour–liquid phase equilibrium relation under the given pressure and liquid concentration, and be independent of boiling conditions. Therefore, the vapour concentration could be obtained by vapour–liquid phase equilibrium relations.

UNIFAC (UNIQUAC Functional-group Activity Coefficients) method, derived from UNIQUAC model by Fredenlund et al. [16] in 1975, performed well for most of higher polar compounds, e.g., water–ethanol mixtures [17]. It was adopted to determine the ethanol concentration of the vapour mixture. Based on this model, a program was developed to calculate the vapour concentration from liquid concentration under different vapour pressures. Under vapour pressure of 6.7 kPa, the computational results of UNIFAC were compared with the experimental data of the literature [18] in Table 1, and they were almost consistent with each other.

2.2.4. The measurement of temperature

The heat transfer flux/coefficient was obtained by calculation from the temperatures in the copper plate and the temperature of vapour. Here thermocouples were used to measure temperatures. In the copper plant, 29 couples of thermocouples were collocated regularly, as shown in Fig. 1(b) (hollow points). From the thermocouples, the temperature field of the plate was obtained. In the condensing chamber, two couples of thermocouples were set to measure the temperature of vapour.

All the data of thermocouples and the pressure transducer were collected by the data acquisition system (NI® PXI-6030E).

2.3. The calculation of heat transfer flux/coefficient

During the experiment, cooling water was heated very slowly and the copper plate was well insulated by a thick Teflon plate from the surroundings, therefore the experimental process could be treated as a two-dimensional, quasi-steady state with no heat generation. The coarse temperature field had been gotten from the thermocouples. To get more precise results, the rectangular region was plotted out. As shown in Fig. 1(b), the hollow points were the thermocouple locations and the solid points were nodes inserted for calculation. Using energy balance method, we could

Table 1
Comparison of experimental data by Gmehling [18] and results of UNIFAC.

Liquid concentration (mol %)	Experimental data by Gmehling [18]		Results of UNIFAC	
	Vapour concentration (mol %)	Phase equilibrium temperature (K)	Vapour concentration (mol %)	Phase equilibrium temperature (K)
6.4	33.20	30.90	39.92	30.13
8.6	40.80	29.40	44.53	28.99
11.1	46.80	28.15	48.18	28.07
14.2	51.20	27.10	51.37	27.26
37.9	63.20	23.90	63.18	24.56
47.8	66.90	23.25	67.18	23.90
78.0	82.20	21.95	82.28	22.48
88.5	89.80	21.70	89.46	22.24

obtain the node temperatures and the heat transfer flux/coefficients. Calculation was performed by the following procedure.

Firstly, the temperatures of the nodes, *ai* ($i = 1, 2, \ldots, 7$), *ci* and *di* ($i = 1, 2, \ldots, 6$), which were midpoints of the testing points, were obtained by extrapolation, such as $T_{a1} = \frac{T_1+T_8}{2}$, $T_{c1} = \frac{T_8+T_9}{2}$, and these values would be revised later. The temperatures of the nodes *bi* ($i = 1, 2, \ldots, 6$) could be computed by energy balance method. For example, for the point b1, the energy equation was that:

$$\phi_w + \phi_n = \phi_e + \phi_s \tag{2}$$

where

$$\phi_w = \lambda \frac{l_{c1-d1}}{2} \frac{T_{a1} - T_{b1}}{l_{a1-b1}}, \quad \phi_n = \lambda \frac{l_{a1-a2}}{2} \frac{T_{d1} - T_{b1}}{l_{d1-b1}},$$
$$\phi_e = \lambda \frac{l_{c1-d1}}{2} \frac{T_{b1} - T_{a2}}{l_{b1-a1}}, \quad \phi_s = \lambda \frac{l_{a1-a2}}{2} \frac{T_{b1} - T_{c1}}{l_{b1-c1}}.$$

From the equations the temperature of *b*1 could be calculated. So were the other points *bi* ($i = 2, 3 \ldots, 6$). Then the temperatures of midpoint nodes could be revised by energy balance method. With the same method the temperatures of *ei* ($i = 1, 2 \ldots, 11$), *fi* ($i = 1, 2 \ldots, 9$) could be calculated. Next the local heat transfer fluxes on the surface were calculated. For example, for the point *f*3, the energy equation was that:

$$\phi_w + \phi_n = \phi_e + \phi_s \tag{3}$$

where

$$\phi_w = \lambda \frac{l_{f3-e4}}{2} \frac{T_{f2} - T_{f3}}{l_{f2-f3}}, \quad \phi_n = \frac{l_{f2-f4}}{2} q_{hf3},$$
$$\phi_e = \lambda \frac{l_{f3-e4}}{2} \frac{T_{f3} - T_{f4}}{l_{f3-f4}}, \quad \phi_s = \lambda \frac{l_{f2-f4}}{2} \frac{T_{f3} - T_{e4}}{l_{f3-e4}}.$$

From the equations the local heat transfer flux of point *f*3 was gotten. The vapour-to-surface temperature difference (ΔT) of point *f*3, which meant the temperature difference between the main vapour and the copper surface at the position *f*3, was that:

$$\Delta T = T_V - T_{f3} \tag{4}$$

The local HTC of point *f*3 was in following:

$$h_{f3} = \frac{q_{hf3}}{\Delta T} \tag{5}$$

The other local HTCs at the positions of *f*2, *f*4, *f*5, *f*6, *f*7 and *f*8 were obtained by the same procedure.

In Eqs. (2)–(4), T_i was the temperature of point *i*, l_{i-j} was distance from point *i* to point *j*, λ was thermal conductivity, and T_V was temperature of vapour, respectively.

2.4. The uncertainty analysis

The experimental data reduction scheme relied on accurate test measurement. The uncertainties, associated with raw measurement and the derived data, were analyzed by the method of Moffat [19]. The uncertainty of heat conductivity (λ) was ±2%, of temperature (T) was ±0.1 °C The distance error between two holes was ±0.5 mm. The resultant uncertainties of heat flux (q) and HTC (h) were ±2.6 ~ 11.4% and ±4.0 ~ 27.2%, respectively.

3. Results and discussion

3.1. The visual observations

During the experiment five known modes, related to the report by Fujji et al. [4], were all observed. The drop drainage process was dynamic, and periodic. Under the same condition, in a circle, the size and quantity of drops was variational in time, as shown in Fig. 4. It could be seen that the drops gradually grew up and united with the increase of time in a circle. When the drop size was to be a certain value, the big drops were united with the others and then were swept down. Meanwhile, the small and dense drops were created and another circle began. The time of a whole circle here was about 0.5 s. The next pictures about the condensation modality were all typical modes in a whole circle. For all mixture vapours, with the increase of ΔT, the condensation modes shifted from smooth film to wavy film, to drop with rivulet, to drop, to drop with rivulet, and to film, as seen in Fig. 5. The condensation

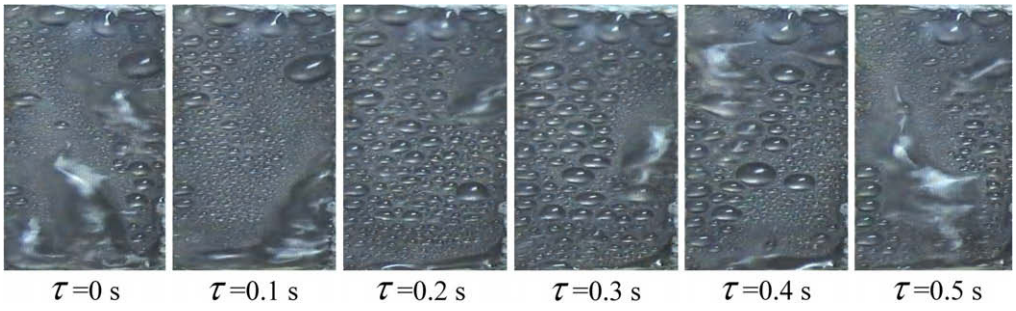

Fig. 4. Variation of condensation modes in time in a circle.

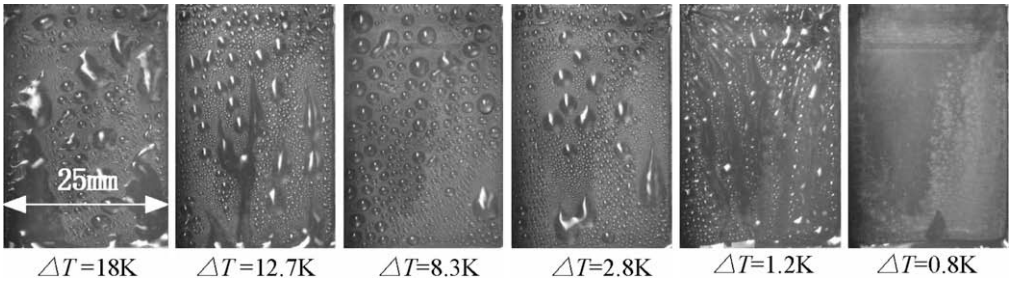

Fig. 5. Condensation modes versus vapour-to-surface temperature difference ($C_V = 2\%$, $P = 47.36$ kPa, $U = 4$ m s^{-1}).

modes greatly depended on EVC and ΔT, as shown in Fig. 6. For pure water, the mode was always film, but with waves on the film at some range of ΔT. For the mixture vapour at low EVCs ($C_V < 5\%$), the ΔT region with drop mode appearance was wide. The size and distribution of drops relied on EVC. At a lower EVC, the drops were smaller and denser. With respect to the effect of EVC and ΔT, the effect of vapour velocity and pressure on condensation modes was weak. Fig. 7 shows the condensation modes observed by Yang et al. [13]. Their experiments were carried out on a vertical surface with uniform temperature. Compared with their condensation modes, the present drops were smaller and denser, and the sweep speed of drops was faster.

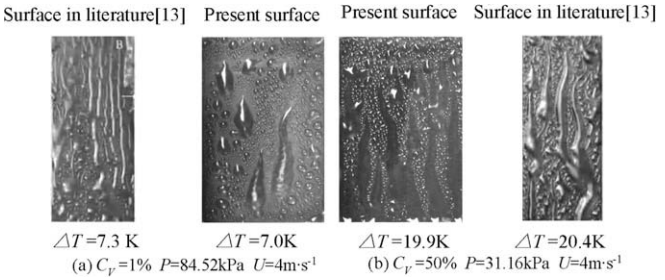

Fig. 7. Comparison of condensation modes for different condensing surfaces.

3.2. Condensation characteristic curves

For the difference of the original intention between the present work and Prof. Utata's work [8–10], the authors thought the present Marangoni condensation driven by solutal effect and thermal effect was a new and unknown task. As reported in Refs. [8–10,13], the ethanol mass fraction, the ΔT, the vapour velocity, and the vapour pressure were all the influencing factors of Marangoni condensation. In order to make clear the heat transfer rules of the present condensation and show the difference between the present condensation and the solutal Marangoni condensation, it was necessary to study the effects of the influencing factors on the present condensation.

Tests were conducted using mass concentrations of ethanol in mixture vapours (C_V) of 0%, 0.5%, 1%, 2%, 5%, 10%, 20% and 50% at three different pressures of 31.16 kPa, 47.36 kPa and 84.52 kPa, respectively, while vapour velocities at approach to the condenser plate were 3 m s^{-1}, 4 m s^{-1} and 6 m s^{-1}, respectively.

According to the calculation in Section 2.3, seven local HTCs (the coefficients at the positions of nodes $f2$–$f8$) could be obtained for the present surface. In view of the symmetry, only three local coefficients at typical positions ($f2$, $f4$ and $f5$) were concerned to study the heat transfer characteristic in this paper.

3.2.1. Effect of temperature gradients on local heat transfer coefficients

Fig. 8 shows the three local HTCs under the same experimental condition. With reference to Fig. 8 we could see that the distinction among the three coefficients was obvious and the coefficient of point $f5$ was lowest, while the coefficient of point $f4$ was highest. Moreover, the distinction greatly depended on EVC and ΔT. At low EVCs ($C_V < 2\%$), the difference values were significant and rose up to be 50 kW m^{-2} K^{-1}, especially at low range of ΔT. When the EVC increased, the difference in value became little and the ΔT region of great distinction moved to large region.

The reason for the difference of local HTCs on condensing surface was attributed to the difference of local surface tension gradients. At the fixed ethanol concentration, the difference of local

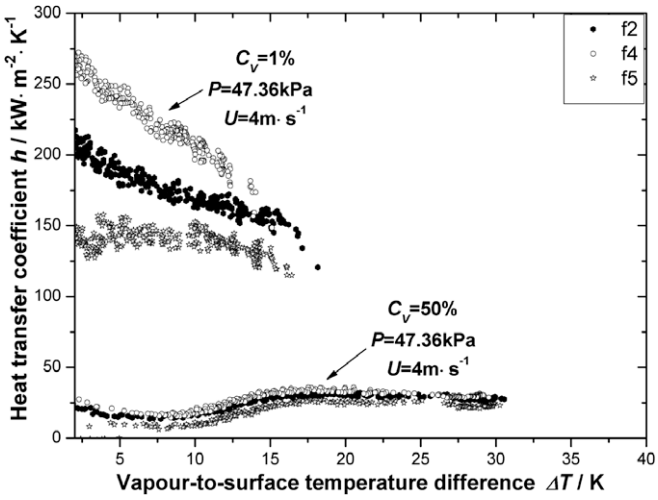

Fig. 8. Comparison of local heat transfer coefficients.

surface tension gradients was mainly due to the different local macroscopical temperature differences, although temperature difference inevitably brought concentration difference. For the special shape, the local temperature differences along the surface were nonhomogeneous. Fig. 9 illustrates the local temperature differences among the nodes. It could be seen that, at the position of node $f4$, the temperature differences were upper, while those of node $f5$ were least. For all ethanol concentrations, the similar conclusion was applied.

Surface tension gradient is the essential driving force of Marangoni convection. It is necessary to research on the relationship between surface tension gradient and temperature gradient. For water–ethanol mixtures, the surface tension was a function of concentration (C), temperature (T), and pressure (P). The data at different pressures were deficient. Moreover, the experiments

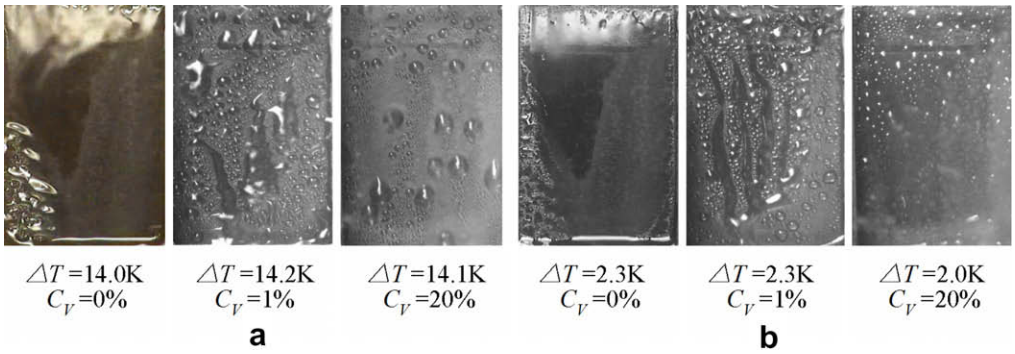

Fig. 6. Condensation modes for difference ethanol vapour concentrations and vapour-to-surface temperature differences.

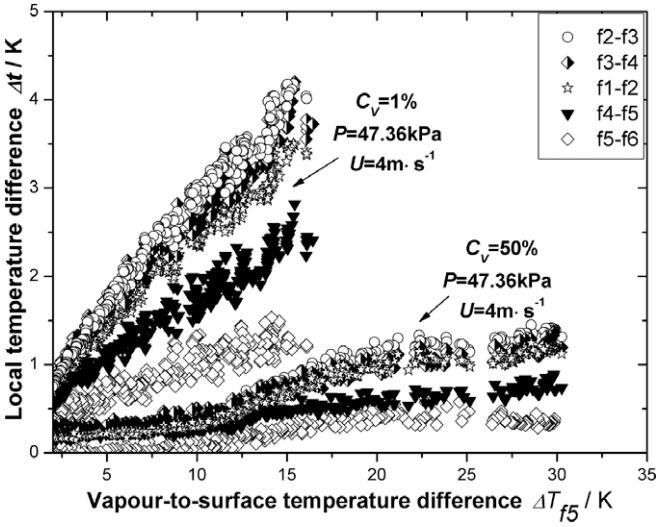

Fig. 9. Comparison of local temperature differences.

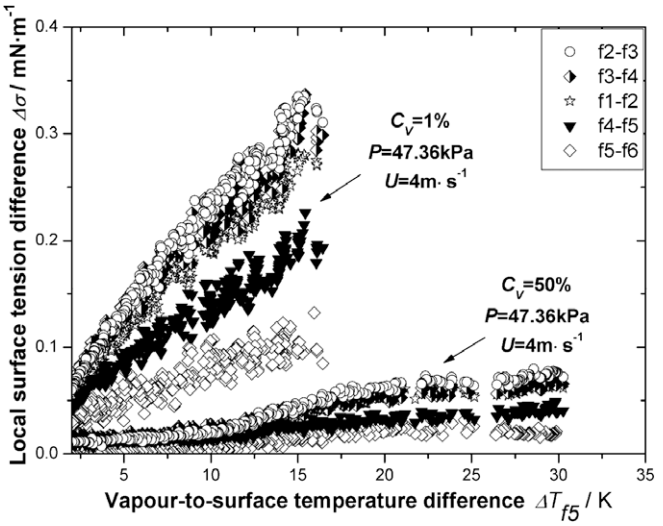

Fig. 10. Comparison of local surface tension differences.

were carried out at adjacent pressures. So for a quantitative comparison at a fixed pressure, the surface tension was just considered to be the function of concentration (C) and temperature (T). The model in Ref. [15] was adopted to calculate surface tension:

$$\sigma = [-0.1649(T-273)+75.973]\left[1-0.411\ln\left(1+\frac{C}{1.37}\right)\right] \quad (6)$$

Table 2 gives the values of experimental data [20], calculation data and error for different concentrations and temperatures. The values calculated by Eq. (6) were in good agreement (error < ±1%) with the experimental values within our discussion. It demonstrated that the fitted Eq. (6) was feasible.

Assuming the interface temperature being a linear relation with the temperature of vapour and condensing surface and the ethanol concentration at the interface obtained by the phase equilibrium relation, the local surface tension differences were calculated using Eq. (6), as shown in Fig. 10. The distinction of local surface tension differences was similar to that of temperature differences. The conclusion was that the local surface tension differences of $f5$ were least and those of $f4$ were upper. As it is known, the Marangoni effect is caused by the surface tension gradients. The larger the surface tension difference is, the stronger Marangoni convection would be. The promotion behavior of Marangoni effect on condensation heat transfer is as follows: Marangoni convection will tear the film and reduce condensate thermal resistance. The diffusion thermal resistance between the vapour and condensate will be also reduced by the disturbance of Marangoni convection. Accordingly, the stronger Marangoni convection reduced more total thermal resistance and the heat transfer was more significant enhanced. So among the points of $f2$, $f4$ and $f5$, the position with the largest temperature difference, $f4$, had the highest HTC, while $f5$ had the least HTC, for least temperature difference.

For mixture vapours, Marangoni convection was driven by surface tension gradient, caused by concentration gradients and temperature gradients. The difference of local HTCs was also the coaction of concentration and temperature gradients.

Expressly, for pure steam, without the effect of concentration gradients, the difference of local HTCs was only the contribution of local temperature gradients on the condensing surface. The difference would show the undoubted effect of temperature gradients on heat transfer.

Fig. 11 shows the present data and the experimental data by Yang et al. [13], whose condensing surface had uniform temperature. Also shown is the Nusselt equation [21] for pure quiescent steam. As seen in Fig. 11, the coefficient in the literature [13] was some higher than the theoretical result, and a little lower than that of node $f5$. The distinction between the coefficients of nodes $f2$ and $f4$ was very little and the coefficient of node $f4$ was just a little higher. But the difference in the coefficients of $f2$ and $f5$ was obvious, up to 30%.

The reason for the difference between Yang and Nusselt was that the experimental vapour was not quiescent and vapour velocity would raise HTC, presumably due to the shear stress effect on the condensate surface.

The latter differences could be the result of the different temperature gradients on the condensing surface. Fig. 12 depicts the local temperature differences and local surface tension differences. The local surface tension differences of $f2$ and $f4$ were larger and

Table 2
Comparison of experimental data in Ref. [20] and results of calculation.

Temperature (K)	Liquid concentration (%)								
	0.25			0.5			1		
	Experimental data (mN m^{-1})	Results of calculation (mN m^{-1})	Error (%)	Experimental data (mN m^{-1})	Results of calculation (mN m^{-1})	Error (%)	Experimental data (mN m^{-1})	Results of calculation (mN m^{-1})	Error (%)
313	67.6	67.3	−0.44	65.3	65.5	0.34	63	62.6	−0.65
323	65.9	65.7	−0.30	63.9	64.0	0.10	61.5	61.1	−0.65
333	64.1	64.1	0.003	62.2	62.4	0.33	60	59.6	−0.64
343	62.6	62.5	−0.15	60.8	60.9	0.08	58.7	58.1	−0.98
353	60.9	60.9	0.004	59.1	59.3	0.33	57.1	56.6	−0.81
363	59.1	59.3	0.34	57.6	57.7	0.24	55.7	55.1	−0.98

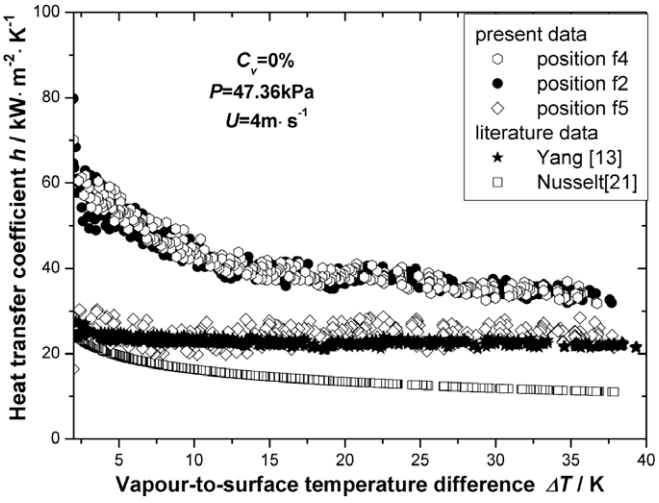

Fig. 11. Heat transfer coefficients for pure steam.

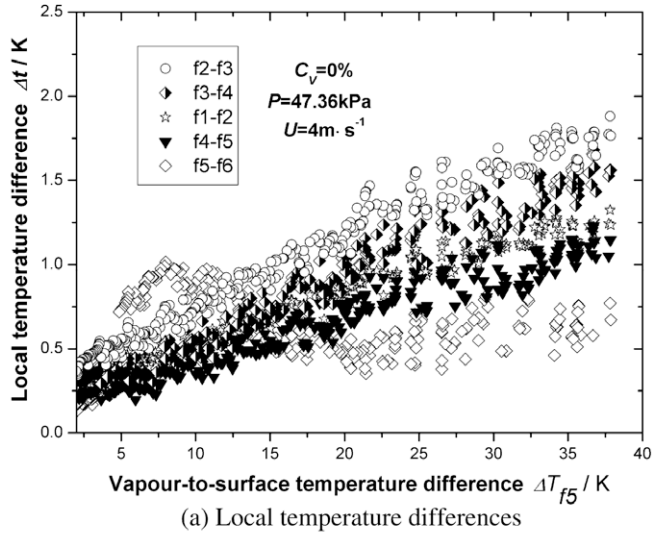

Fig. 12. Comparison of local temperature and surface tension differences for pure water.

those of *f*5 were lower, just more than zero. The local temperature difference on Yang's condensing surface was thought to be zero. Then, at the position of *f*4 and *f*2 with much larger surface tension differences, the coefficients were higher than others. At the position of no local temperature difference the coefficient was least.

The condensate mode also confirmed the effect of temperature gradients. From the pictures of condensation modes of pure steam, as seen in Fig. 6, the film with ripples could be observed obviously. The Marangoni convection caused by temperature gradients was existent to enhance heat transfer, but too weak to tear the film.

3.2.2. Effect of ethanol vapour concentration on heat transfer coefficients

The results are shown in Fig. 13 in the form of graphs of HTC versus ΔT. From Fig. 13, when the EVC was at low range (C_V = 0.5%, 1%), the variation trends of HTCs with the increase of ΔT were similar. The HTC always decreased with the increase of ΔT, and the decrease rate would change at a certain ΔT and then became relaxative. When the EVC was higher ($C_V \geqslant 2\%$), the heat transfer characteristic curves were similar. The characteristic curve was a nonlinear curve with a maximum: the HTC kept on a lower value at low ΔT, then increased with the increase of ΔT steeply, after being to the maximum, the HTC decreased with increasing ΔT. Under the same condition, the highest HTC appeared at the EVC of 1%. The HTC of EVC of 0.5% was a little lower with respect to 1%. When the EVC was higher than 2%, the HTC decreased with increasing concentrations. The coefficient of EVC of 20% was lower than that of pure steam when ΔT was less than 12 K, but much higher than that of pure steam at the ΔT range of more than 12 K. The coefficient of EVC of 50% was always lower than that of pure steam.

3.2.3. Effect of temperature gradients on heat transfer

As shown above, the HTCs were diverse along the condensing surface. A mean heat transfer coefficient was introduced for the sake of comparison, and could be expressed as

$$\bar{h} = \frac{\bar{q}}{\Delta\bar{T}} = \frac{\int_0^l q dx}{\int_0^l \Delta T dx} \tag{7}$$

Fig. 14 delineates the variation trend of mean HTC versus mean ΔT. In the figure also shown are the results of Yang et al. [13]. Inspection of Fig. 14 showed that the variation trends of HTCs with ΔT were similar with the literature data, except for the low EVCs (C_V = 0.5%, 1%). The condensation characteristic curves of low EVCs were seen as the latter half part of those of higher concentrations. The first half part of curves, including the part of low values and steep increase part, was nonexistent. For the precision restriction of experimental equipment, the experimental data were deleted when ΔT was less than 2 K. Considering the thermal resistance analysis of Ref. [8] and the change trends of other concentrations, it might be concluded that the first half parts of curves should be at the ΔT region of less than 2 K, when the EVC was 0.5% and 1%, respectively. Another likely reason may be that the temperature gradients made the ΔT region move to low range and the first half parts of curves were short and fell into oblivion. The results showed that the present heat transfer coefficients were significant high at low range of ΔT, for the mixture vapours with a low ethanol concentration. In engineering application, the usual ΔT was always low. So the present findings were of great benefit to obtaining significant heat transfer enhancement in engineering application.

The second difference between the two researches was that the present HTC of EVC of 0.5% was just lower than that of 1%, while in the former data the coefficient of 2% was the second highest.

As seen in Fig. 14, compared with the heat transfer of solutal Marangoni condensation, the present data were much higher for

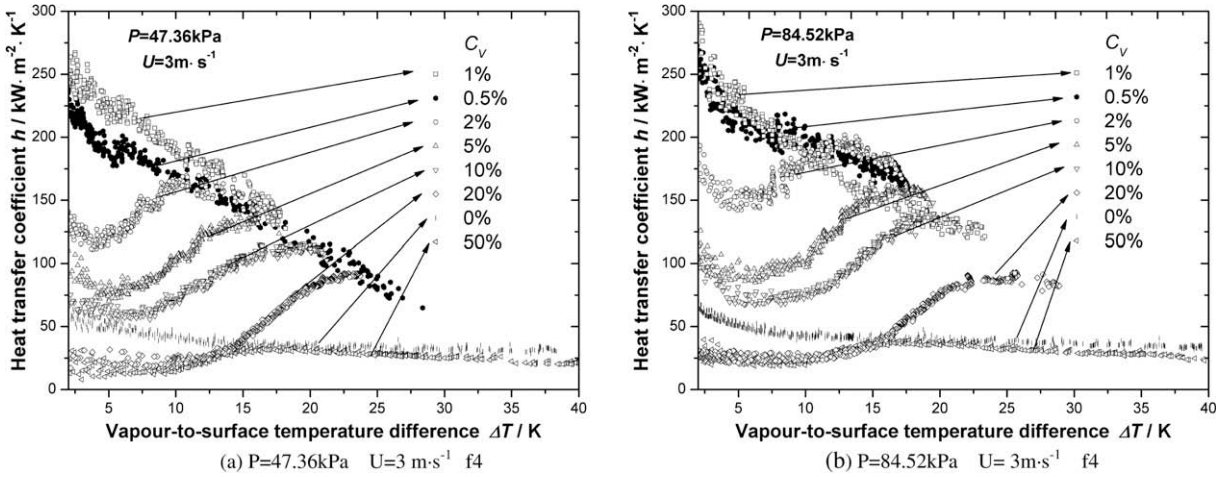

Fig. 13. Heat transfer coefficients for different ethanol vapour concentrations.

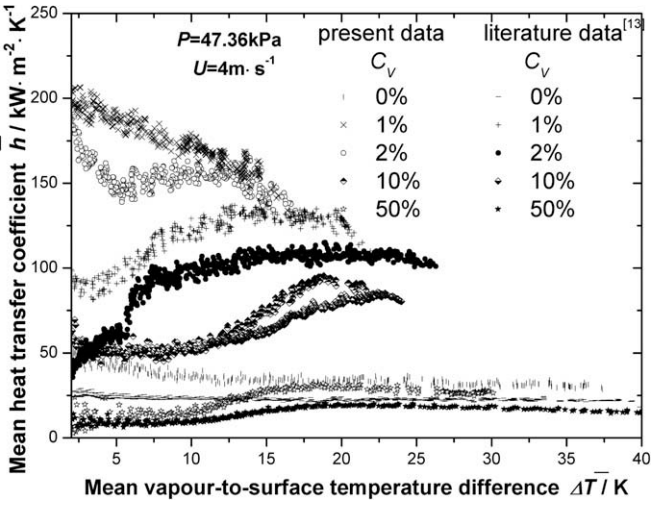

Fig. 14. Comparison of present data with Yang et al. [13].

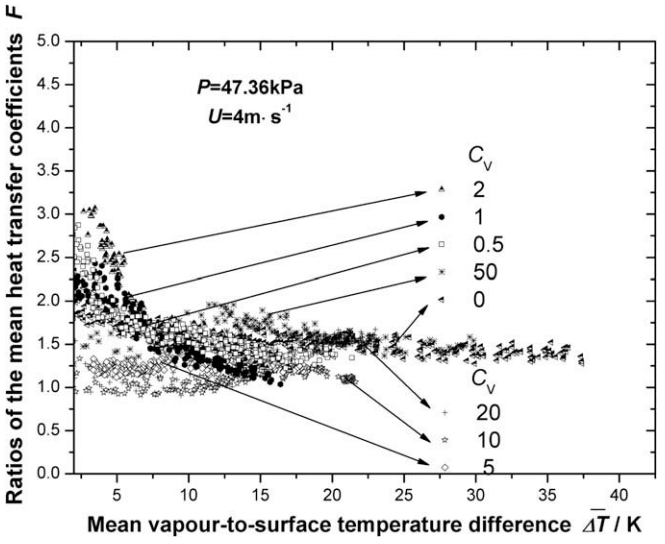

Fig. 15. Ratios of the present condensation mean heat transfer coefficients to those of Yang et al. [13].

full range of ethanol concentrations. For pure steam, the heat transfer was enhanced approximately by 50% for the existence of temperature gradients on the surface. For the mixture vapours of low ethanol concentrations, the difference between the two condensation behaviors was distinct, especially at the low range of ΔT. The maximum value reached to 100 kW m^{-2} K^{-1}. The difference values decreased rapidly with the increase of ΔT. When the concentration was higher, the difference between the two condensation behaviors became little, and the range of ΔT with maximum difference changed to the higher range.

Fig. 15 presents the ratios of the present condensation HTCs to those of Yang et al. [13]. The ratios were always more than 1. At the low EVCs (C_V < 5%), including the pure steam, the ratios were mostly 1.25–2, even 2–3 at low range of ΔT. For higher concentrations the ratios were mostly between 1 and 1.5. For the EVC of 50%, the ratio was again between 1.25 and 2. The comparison showed that, at the low EVCs ($0 \leqslant C_V < 5\%$) and very high EVC ($C_V = 50\%$), the heat transfer was further enhanced by 25–100%; at the middle EVC range, the heat transfer was further enhanced by 0–50%. The more powerful heat transfer enhancement was the contribution of the macroscale temperature gradients on the condensing surface. On the basic of the concentration gradients, the temperature gradients induced more powerful Marangoni convection. The total thermal resistance was decreased and the heat transfer was further enhanced.

3.2.4. Effect of vapour velocity on heat transfer

Referring to Refs. [12,13], three vapour velocities, 3 m s^{-1}, 4 m s^{-1} and 6 m s^{-1}, were adopted. As the similar law in the previous studies [9], the mean HTCs increased with the increase of vapour velocities, as shown in Fig. 16. The influence degree was close relative to the EVC: strong at low concentrations and weak at high concentrations. The enhancing effect of vapour velocity was presumably due to the reduction of diffusion resistance in the vapour-side and the thermal resistance in condensate as well as to the shear stress effect on the condensate surface.

3.2.5. Effect of vapour pressure on heat transfer

Little attention was paid to the effect of vapour pressure on Marangoni condensation before. Our tests were conducted at three pressures: 31.16 kPa, 47.36 kPa and 84.52 kPa, respectively. The HTCs at different pressures are shown in Fig. 17. The effect of vapour pressure on heat transfer was positive and the rate of increase of heat transfer depended on EVC and ΔT. The sensitivity to pressure became less at higher EVCs. For the physical properties of mixture vapour, the condensing rate increased with increasing pressure. The result was that the falling speed was faster at high pressure and the disorder between vapour and condensate became

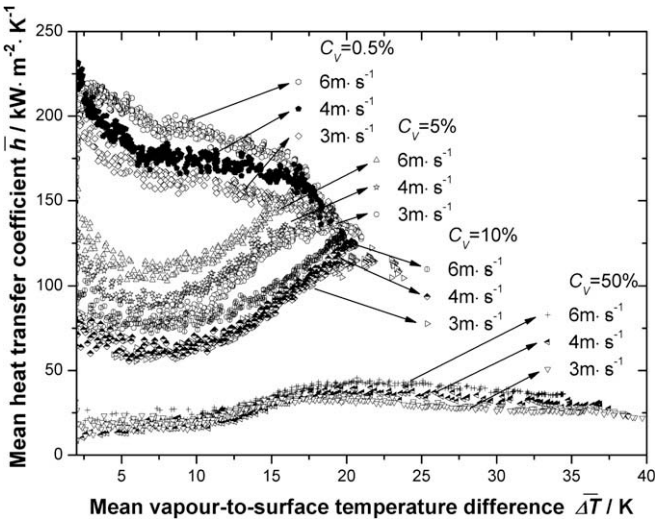

Fig. 16. Mean heat transfer coefficient versus mean vapour-to-surface temperature difference at various velocities (P = 84.52 kPa).

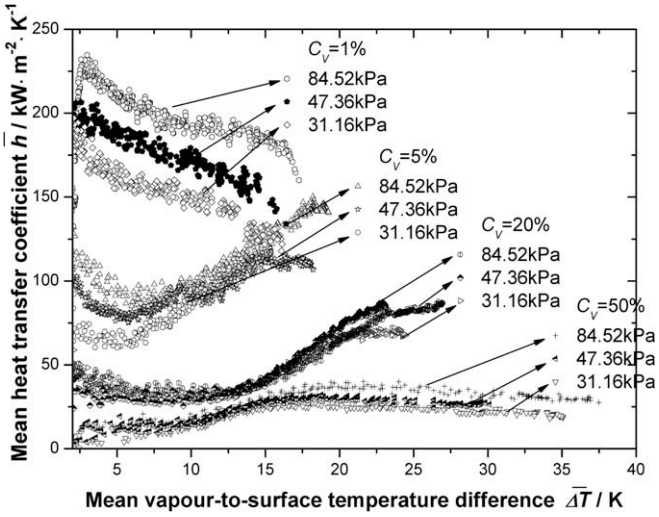

Fig. 17. Mean heat transfer coefficient versus mean vapour-to-surface temperature difference at various pressures (U = 4 m s^{-1}).

stronger. Then the diffusion resistance and thermal conduction resistance both decreased and heat transfer increased.

4. Preliminary analysis of the effect of the coactions of temperature and concentration gradients

The present pseudo-dropwise condensation was the result of Marangoni convection, which was caused by surface tension gradients for concentration and temperature gradients. This section discussed the effect of the coactions of temperature and concentration gradients on Marangoni condensation heat transfer.

As the condensate of water–ethanol mixture is a positive system, the relation between surface tension and ethanol concentration is that

$$\left(\frac{\partial\sigma}{\partial C}\right)_{sat} < 0 \tag{8}$$

The relation between ethanol concentration and temperature is that

$$\left(\frac{\partial C}{\partial T}\right)_{sat} < 0 \tag{9}$$

as ethanol is a volatile component. Then the relation between surface tension and temperature can be obtained as follows:

$$\left(\frac{\partial\sigma}{\partial T}\right)_{sat} \equiv \left(\frac{\partial\sigma}{\partial C}\right)_{sat}\left(\frac{\partial C}{\partial T}\right)_{sat} > 0 \tag{10}$$

From relation (8) it can be concluded that the surface tension gradients by ethanol concentration gradients point from the high ethanol concentration region to the low concentration region. From relation (10) we can induce that the surface tension gradients caused by temperature gradients point from the high temperature region to the low temperature region. A conclusion obtained from relation (9) is that the high temperature region has higher ethanol concentration. So we can find the direction of surface tension gradients by temperature gradients is the same with that by concentration gradients in the present work.

Because of the coupling of temperature and concentration, the bulk temperature gradient on the condensing surface will cause great concentration distribution. It means the solutal effect will be strengthened. According to the conclusion obtained above, the surface tension gradients on the saturated condensate surface become greater under the coactions of the solutal and thermal effects, caused by concentration and temperature gradients. Compared with the solutal Marangoni condensation, the present Marangoni condensation is thought to be added a driving force. As a result, Marangoni convection becomes more vigorous, leading to the condensation heat transfer to be further enhanced.

5. Conclusions

The Marangoni condensation heat transfer on a vertical surface with larger and nonhomogeneous temperature gradients was researched experimentally in this paper. The visual observations indicated that condensation modes greatly depended on EVC and ΔT. The investigation results are summarized as follows:

(1) For the nonhomogeneous temperature gradients on condensing surface, leading to nonhomogeneous surface tension gradients, the local HTCs were varied along the condensing surface. The HTC was higher at the position with greater local temperature gradients.
(2) The highest HTC occured at the EVC of 1%. The coefficient of EVC of 0.5% was just lower than that of EVC of 1%. The heat transfer coefficient decreased with the increase of EVC when the EVC was more than 2%.
(3) For the effect of temperature gradients, the present condensation heat transfer was further enhanced. Compared to the solutal Marangoni condensation, for the low EVCs ($0 \leqslant C_V < 5\%$) and the very high EVC (C_V = 50%), the heat transfer was enhanced by 25–100%. At the middle EVC region, the enhancing ratio was smaller, about 0–50%.
(4) The HTC increased with the increase of vapour velocity and pressure, and the sensitivity depended on the EVC and ΔT.
(5) The preliminary analysis shows that, for a positive system with a volatile component, under the coaction of concentration and temperature gradients, the surface tension gradient on the condensate surface becomes greater, leading to the Marangoni condensation heat transfer to be further enhanced.

Acknowledgements

The authors thank Prof. Y. Utaka at Yokohama National University, for his experimental assistance and academic discussion. This project has been supported by National Natural Science Foundation of China through Grant Nos. 50476048 and 50521604.

References

[1] V.V. Mirkovich, R.W. Missen, Non-filmwise condensation of binary vapor of miscible liquids, Can. J. Chem. Eng. 39 (1961) 86–87.

[2] F.G. Tenn, R.W. Missen, A study of the condensation of binary vapors of miscible liquids. Part 1: The equilibrium relations, Can. J. Chem. Eng. 41 (1963) 12–14.

[3] J.D. Ford, R.W. Missen, On the conditions for stability of falling films subject to surface tension disturbances, the condensation of binary vapors, Can. J. Chem. Eng. 48 (1968) 309–312.

[4] T. Fujii, N. Osa, S. Koyama, Free convection condensation of binary mixtures on a smooth tube: condensing mode and heat transfer coefficient of condensate, in: Proceedings of the Engineering Foundation Conference on Condensation and Condenser Design, St. Augustine, Florida, ASME, 1993, pp. 171–182.

[5] K. Hijikata, Y. Fukasaku, O. Nakabeppu, Theoretical and experimental studies on the pseudo-dropwise condensation of a binary vapor mixture, J. Heat Transfer 118 (1996) 140–147.

[6] J.N.A. Morrison, J. Deans, Augmentation of steam condensation heat transfer by addition of ammonia, Int. J. Heat Mass Transfer 40 (1997) 765–772.

[7] C. Philpott, J. Deans, The enhancement of steam condensation heat transfer in a horizontal shell and tube condenser by addition of ammonia, Int. J. Heat Mass Transfer 47 (2004) 3686–3693.

[8] Y. Utaka, N. Terachi, Measurements of condensation characteristic curves for binary mixture of steam and ethanol vapor, Heat Transfer Jpn. Res. 24 (1995) 57–67.

[9] Y. Utaka, H. Kobayashi, Effect of velocity on condensation heat transfer for steam–ethanol binary vapor mixture, in: Proceedings of the Sixth ASME–JSME Thermal Engineering Joint Conference, CD paper TED-AJ03-604, 2003.

[10] Y. Utaka, S. Wang, Characteristic curves and promotion effect of ethanol addition on steam condensation heat transfer, Int. J. Heat Mass Transfer 47 (2004) 4507–4516.

[11] T. Murase, H.S. Wang, J.W. Rose, Marangoni condensation of steam–ethanol mixtures on a horizontal tube, Int. J. Heat Mass Transfer 50 (2007) 3774–3779.

[12] J.J. Yan, Y.S. Yang, S.H. Hu, et al., Effects of vapor pressure/velocity and concentration on condensation heat transfer for water–ethanol mixture, Heat Mass Transfer 44 (2007) 51–60.

[13] Y.S. Yang, J.J. Yan, X.Z. Wu, et al., Effects of vapor pressure on Marangoni condensation of steam–ethanol mixtures, J. Thermophys. Heat Transfer 22 (2008) 247–253.

[14] Y. Utaka, T. Kamiyama, Condensate drop movement by applying bulk temperature gradient on heat transfer surface in Marangoni condensation, Trans. Jpn. Soc. Mech. Eng. B 73 (2007) 2530–2536 (in Japanese).

[15] S.H. Hu, J.J. Yan, J.S. Wang, Effect of temperature gradient on Marangoni condensation heat transfer for ethanol–water mixtures, Int. J. Multiphase Flow 33 (2007) 935–947.

[16] Aa. Fredenlund, R.L. Jones, J.M. Prausnitz, Group contribution estimation of activity coefficients in non-ideal liquid mixtures, AIChE J. 27 (1975) 1086–1099.

[17] A.F. Claudio, J.O. Valderrama, Phase equilibrium modeling in binary mixtures found in wine and must distillation, J. Food Eng. 65 (2004) 577–583.

[18] J. Gmehling, Vapor–liquid equilibrium data collection. Organic hydroxy compounds: alcohol and phenols, in: Chemistry Data Series 1: Part 2a, Frankfurt, 1978.

[19] R.J. Moffat, Contributions to the theory of single-sample uncertainty analysis, J. Fluids Eng., Trans. ASME 104 (1982) 250–260.

[20] G.Q. Liu, L.X. Ma, Handbook of Chemical Engineering Calculations, Chemical Industry Press, 2002.

[21] W. Nusselt, Die Oberflachenkodensation des Wasserdampfes, Z. Vereines Deutsch. Ing. 60 (1916) 569–575.